

## RESEARCH ARTICLE

# Effects of Water and Polymer Content on Covalent Amide-Linked Adduct Formation in Peptide-Containing Amorphous Lyophiles

Michael P. DeHart,<sup>1</sup> Bradley D. Anderson<sup>2</sup>

<sup>1</sup>Catalent Pharma Solutions, 1100 Enterprise Drive, Winchester, Kentucky 40391

<sup>2</sup>Department of Pharmaceutical Sciences, College of Pharmacy, University of Kentucky, Lexington, Kentucky 40536-0082

Received 4 October 2011; revised 16 January 2012; accepted 7 February 2012

Published online in Wiley Online Library (wileyonlinelibrary.com). DOI 10.1002/jps.23092

**ABSTRACT:** Deamidation of asparagine-containing proteins and peptides results in the formation of hydrolysis products via a reactive succinimide intermediate. In amorphous lyophile formulations at low water content, nucleophilic amine groups in neighboring molecules can effectively compete with water for reaction with the succinimide intermediate resulting in the formation of a variety of covalent amide-linked adducts. This study examines the effects of changes in percentage of a polymeric excipient [hypromellose (HPMC)] and water content on the degradants formed from a model asparaginyl peptide (Gly-Phe-L-Asn-Gly) in amorphous solids also containing an excess of Gly-Val and carbonate buffer and stored at 40°C. Degradation of Gly-Phe-L-Asn-Gly and formation of succinimide intermediates, aspartyl peptides, and covalent amide-linked adducts were monitored by high-performance liquid chromatography. In all formulations and storage conditions, the formation kinetics of aspartyl hydrolysis products and covalent adducts could be described by a mechanism-based model that assigned a central role to the succinimide intermediate. Increasing the percentage of HPMC (i.e., reactant dilution) favored the formation of hydrolysis products over covalent amide-linked adducts, consistent with the bimolecular nature of covalent adduct formation. Increases in water content as relative humidity (RH) was varied from 33% to 75% produced orders-of-magnitude increases in the rate constants for succinimide formation and hydrolysis with both becoming nearly constant at high water contents. A bell-shaped profile for the dependence of the rate of covalent adduct formation on water content was observed, a result that may be indicative of phase separation at higher RHs. © 2012 Wiley Periodicals, Inc. and the American Pharmacists Association *J Pharm Sci*

**Keywords:** amorphous; chemical stability; deamidation; hypromellose; lyophilization; nondispersible aggregates; solid-state stability; peptide stability; phase separation; protein aggregation

## INTRODUCTION

Peptides and proteins are inherently unstable in solution and are therefore generally formulated as lyophilized solids to maximize their stability. Amorphous lyophiles stored below the glass transition temperature ( $T_g$ ) of the system exist as glasses in which local molecular reorientations (i.e., local mobility or  $\beta$ -relaxation) dominate, whereas long-range molecular motions (i.e., global mobility or  $\alpha$ -relaxation) are retarded. In recent years, the im-

portant role of molecular motions in inducing instability even at temperatures well below  $T_g$  has become increasingly appreciated.<sup>1–5</sup> In turn, this has led to numerous attempts to relate decreases in stability that accompany increases in temperature and relative humidity (RH) to various measures of molecular mobility such as the  $T_g$  itself or relaxation times determined using methods such as differential scanning calorimetry,<sup>5–7</sup> isothermal calorimetry,<sup>8</sup> thermally stimulated depolarization current spectroscopy,<sup>9</sup> dielectric spectroscopy,<sup>10,11</sup> thermomechanical analysis,<sup>12</sup> or nuclear magnetic resonance.<sup>13</sup> Empirical equations that were originally developed to account for the temperature dependence of structural relaxation in amorphous systems including the Williams–Landel–Ferry equation,<sup>14,15</sup> the Adam–Gibbs–Vogel equation,<sup>15</sup> and

Additional Supporting Information may be found in the online version of this article. Supporting Information

Correspondence to: Bradley D. Anderson (Telephone: +859-218-6536; Fax: +859-257-2489; E-mail: bande2@uky.edu)

*Journal of Pharmaceutical Sciences*

© 2012 Wiley Periodicals, Inc. and the American Pharmacists Association

the Kohlrausch–Williams–Watts equation<sup>16–19</sup> are now frequently utilized in the pharmaceutical literature to relate chemical degradation to temperature.

Yet, despite these trends, a number of cases cited in the literature have shown a lack of correlation between reactivity and  $T_g$ <sup>20,21</sup> or other measures of molecular mobility.<sup>22</sup> One possible explanation is that different types of mobility may be responsible for different types of reactions.<sup>23</sup> For example, chemical reactions requiring translational diffusion of large molecules may be more closely coupled with measures of global mobility or long-range structural relaxation, whereas intramolecular reactions may be sensitive only to local reorientations.<sup>9,22</sup>

Often ignored in attempts to establish the degree of coupling between the kinetics of a chemical reaction in amorphous solids and a particular relaxation parameter is the fact that most reactions of pharmaceutical interest involve multiple reaction steps. For example, most of the important degradation pathways for proteins and peptides including deamidation, isomerization, and racemization<sup>24</sup>; covalent aggregate formation involving disulfide,<sup>25,26</sup> amide,<sup>27–30</sup> or lysinoalanine cross-links<sup>31</sup>; oxidation<sup>32,33</sup>; and the Maillard reaction<sup>34</sup> all occur through one or more reactive intermediates. Deamidation of asparagine residues in proteins and peptides occurs via a succinimide intermediate, in both aqueous solutions<sup>24,27</sup> and amorphous lyophiles.<sup>35,36</sup> Recently, we demonstrated that the decomposition of a model asparagine-containing peptide in amorphous lyophiles containing an excess of a second peptide (Gly–Val) produced at least 10 degradants including products from hydrolysis, isomerization, and racemization reactions as well as four amide-linked covalent adducts.<sup>37</sup> Application of a mechanism-based model to fit the kinetic data established that the rate-determining step in the reaction was the formation of a reactive succinimide and that the formation of all subsequent degradation products proceeded through the succinimide.<sup>37</sup>

Mechanistic models that take into account the detailed reaction chemistry, when known, may be useful tools in understanding how changes in formulation and storage conditions might impact amorphous product stability and the degradants generated. It is likely that such models may provide more clarity in understanding the role of structural relaxation in chemical stability by allowing one to explore the degree of coupling of each reaction step to various types of relaxation parameters. In this study, formulations containing the model peptide, Gly–Phe–L–Asn–Gly, in the presence of an excess of a second peptide (Gly–Val) were chosen as a model system to explore the effects of RH and varying percentages of a polymeric excipient [hypromellose (HPMC)] on both the rate of succinimide formation and the competition between two nucleophilic components in the formulation (water and

the N-terminus of Gly–Val) for the reactive intermediate. Bulking agents such as sugars<sup>38</sup> or polymers<sup>39,40</sup> are commonly used in protein and peptide lyophilized formulations to minimize aggregation or recrystallization. HPMC was chosen for this study because of its ability to prevent recrystallization of active ingredients,<sup>41</sup> its relatively high  $T_g$ ,<sup>42</sup> and because the majority of its hydroxyl groups have been alkylated, thus minimizing the number of potential nucleophilic sites on the excipient. We have previously shown that covalent adducts between Gly–Phe–L–Asn–Gly and the N-terminus of Gly–Val are produced exclusively from the succinimide intermediate.<sup>37,43</sup> The results presented in this manuscript illustrate the value of a mechanism-based model for understanding the effects of formulation variables and storage conditions on both the overall rate of degradation and the degradants produced.

## MATERIALS AND METHODS

### Reagents

The starting reactant, Gly–Phe–L–Asn–Gly, and corresponding hydrolysis products were synthesized by GenScript (Piscataway, New Jersey) as trifluoroacetate salts with purities greater than 95% as determined by high-performance liquid chromatography (HPLC). These compounds were further characterized as previously described.<sup>37</sup> Standards of succinimide intermediates (Gly–Phe–D–Asu–Gly and Gly–Phe–L–Asu–Gly) and covalent adducts used for HPLC quantitation are described elsewhere.<sup>37</sup> A sample of HPMC (Methocel E5), having an average substitution of 29% methyl and 10% propyl groups, was donated by Dow Chemical (Midland, Michigan) and used as received. Gly–Val was purchased from Bachem (Torrance, California) as the zwitterion (99.0% purity by thin layer chromatography). HPLC-grade acetonitrile was purchased from Fisher Scientific (Springfield, New Jersey). Sodium bicarbonate (ACS grade) was purchased from EM Science (Gibbstown, New Jersey), and succinic acid was purchased from Aldrich (St. Louis, Missouri). Anhydrous dimethylsulfoxide (DMSO) used in determining water content was purchased from Acros Organics (Pittsburgh, Pennsylvania). Deionized water was used throughout the experiments.

### Preparation of Lyophiles

Preparation and characterization of lyophiles from a 0.5% HPMC solution were previously described in detail. Similarly, solutions of HPMC at higher concentrations [1.0%, 1.5%, 2.0%, 3.0% (w/v)] were prepared by adding the appropriate amount of polymer to buffered solutions (pH adjusted to 9.5 with dilute sodium hydroxide) containing sodium

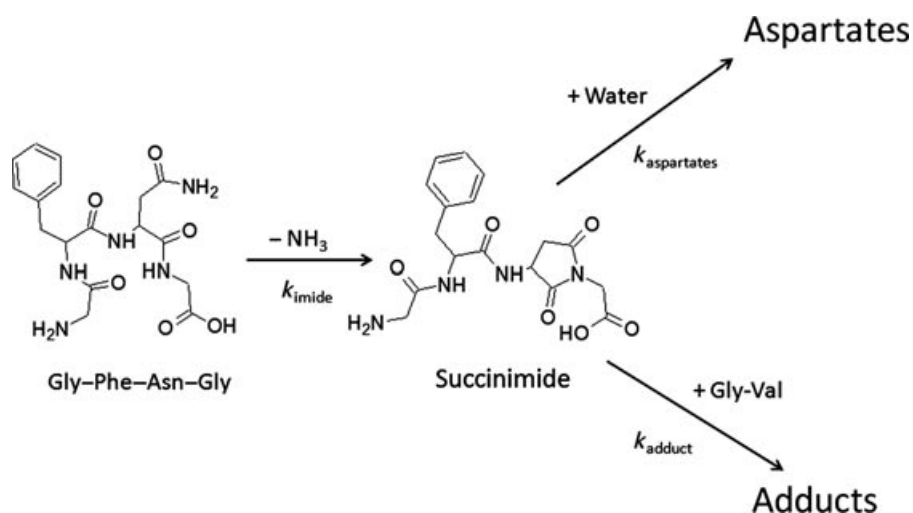


**Figure 1.** Reaction mechanism reflected in the kinetic model (Eqs. 1–4) used to generate rate constants for the formation of the succinimide intermediate from Gly-Phe-L-Asn-Gly, and the formation of aspartates or amide-linked covalent adducts from the reaction of the succinimide with water or Gly-Val, respectively.

bicarbonate (9.3 mM) and Gly-Val (1.5 mM). Gly-Phe-Asn-Gly was then added to buffer/polymer solution to make a 1 mM solution. The peptide solution was mixed, and 100  $\mu\text{L}$  aliquots were transferred into glass autosampler vials. Vials were then placed on a prechilled lyophilization shelf ( $-45^\circ\text{C}$ ) to freeze the samples. Once the samples were frozen (approximately 5–8 min), the lyophilization cycle was initiated. The lyophilization cycle consisted of primary drying at  $-40^\circ\text{C}$  for 1420 min followed by an increase in shelf temperature at a rate of  $0.2^\circ\text{C}/\text{min}$  to  $40^\circ\text{C}$ . Secondary drying at  $40^\circ\text{C}$  was completed after 120 min. The pressure was held constant at 100 mtorr throughout the run.

Lyophiles for water determination were prepared by transferring 2 mL aliquots into 20-mL scintillation vials followed by lyophilization using the same cycle as above. These lyophiles were then dried further in a vacuum oven at  $50^\circ\text{C}$  for 4 days or until the weight remained constant, then analyzed for water content as described below.

### Kinetic Studies

All kinetic studies were performed at  $40^\circ\text{C}$ . Lyophiles prepared from a 0.5% (w/v) solution of HPMC were exposed to various RHs by storing the lyophiles over saturated salt solutions of sodium chloride (75% RH), sodium nitrate (60% RH), potassium carbonate (40% RH), and magnesium chloride (33% RH).<sup>44</sup> Lyophiles containing higher percentages of HPMC were all stored at the same RH (40%).

Initially, lyophiles were preequilibrated at ambient temperature and at the same RH to be employed in kinetic studies for as little as 15 min (75% and 60% RH) or as long as 12 h (40% and 33% RH). This preequilibration step was deemed necessary to ensure that wa-

ter content became constant prior to initiating kinetic studies at  $40^\circ\text{C}$ . After the preequilibration step, samples were placed in a desiccator at the same RH and  $40^\circ\text{C}$  and the time ( $T_{\text{zero}}$ ) was recorded. Samples were removed at specific time points, diluted with deionized water along with a few microliters of 1 N HCl to adjust pH to approximately 4.1 to quench the reaction and provide a similar pH value as the mobile phase. Samples were then analyzed immediately or placed in a freezer ( $-20^\circ\text{C}$ ) until the time of analysis.

The reactant and degradant concentrations were monitored versus time using a stability-indicating HPLC method during a time frame in which <25% of the starting reactant degraded. Mass balance remained at >95% throughout this time frame. Concentrations of the individual succinimide intermediates, hydrolysis products, and covalent adducts obtained from peak areas and response factors generated from standards were pooled and labeled as “succinimides,” “aspartates,” and “adducts.” These pooled concentrations versus time were then analyzed simultaneously using a mechanism-based kinetic model. Figure 1 illustrates the assumed mechanism for the formation of the succinimide intermediate from the starting asparagine-containing peptide followed by its reaction with water or Gly-Val to form aspartates or amide-linked covalent adducts, respectively. Differential equations (Eqs. 1–4) were derived based on Figure 1 to fit the concentration versus time using nonlinear regression software (Scientist; Micromath Scientific Software, St. Louis, Missouri).

$$\frac{\partial [\text{Gly} - \text{Phe} - \text{L} - \text{Asn} - \text{Gly}]}{\partial t} = -k_{\text{succinimide}} [\text{Gly} - \text{Phe} - \text{L} - \text{Asn} - \text{Gly}] \quad (1)$$

$$\frac{\partial [\text{Succinimide}]}{\partial t} = k_{\text{succinimide}} [\text{Gly} - \text{Phe} - \text{L} - \text{Asn} - \text{Gly}] - (k_{\text{aspartates}} + k_{\text{adducts}}) [\text{succinimide}] \quad (2)$$

$$\frac{\partial [\text{Aspartates}]}{\partial t} = k_{\text{aspartates}} [\text{succinimide}] \quad (3)$$

$$\frac{\partial [\text{Adducts}]}{\partial t} = k_{\text{adducts}} [\text{succinimide}] \quad (4)$$

## Lyophile Characterization

### Water Content

Post-lyophilization samples were prepared for the analysis of water content by suspending the entire cake in anhydrous DMSO (~1 mL). The water content was measured by injecting the suspension into the cell of a Karl Fischer apparatus. Carbonate buffers contribute a molar amount of water to the measured water content.<sup>45</sup> The contribution of carbonate buffer was subtracted from the measured water content to obtain initial water contents for each formulation. A brief validation study was performed to confirm that carbonate contributes a molar equivalent when analyzed by Karl Fischer titration. Lyophiles containing varying weight ratios of sodium bicarbonate to Gly-Val (0:1, 1:1, 2:1, and 3:1) were prepared and analyzed as stated above. Once adjusting for the molar equivalent of water contributed by the carbonate buffer, the water contents for each of the lyophiles were equivalent.) The water contents for lyophiles stored at various RHs were determined by monitoring their change in weight, which was attributed to water uptake. These results were then added to the initial sample water contents to obtain the values reported.

### Reconstituted Solution pH

Lyophiles were reconstituted with 100  $\mu$ L of water, and the pH was measured at the beginning and end of the kinetic experiments. An averaged value is reported as the experimental value. Measurements were performed using a Beckman PHI 40 pH Meter (Brea, California) with a MI-40 combination micro-pH probe (Microelectrodes, Inc., Bedford, New Hampshire).

### Polarized Light Microscopy

Samples of each formulation were analyzed by polarized light microscopy at the beginning and end of the kinetic studies. Cakes were suspended in silicone oil, placed on a glass slide, and then covered with a glass cover slip. Samples were then examined for crystallinity using a polarizing microscope (Olympus BX51, Olympus Corporation, Center Valley, Pennsylvania) equipped with a 522 nm filter.

## RESULTS

### Lyophile Characterization

#### Appearance and pH

Lyophiles of each formulation after lyophilization were white and retained the height of the original fill volume. Lyophiles stored at 75% RH were partially collapsed (approximately 50% of their original height) after the initial equilibration step at ambient temperature. No further collapse was observed when these samples were transferred to chambers at the same RH at 40°C. Lyophiles stored at RHs below 75% showed no evidence of collapse. The absence of any detectable birefringence when lyophiles were viewed under a polarizing microscope (data not shown) indicated that none of the formulation components crystallized to an extent that could be visualized by this method. The pH values of reconstituted formulations before and after the kinetic studies were not significantly different.

#### Water Content and Composition at Varying RH

A summary of the water content in lyophiles varying in the amounts of HPMC incorporated into the formulations is shown in Table 1. Percentages of HPMC and the other formulation components listed in Table 1 were calculated on the basis of the water content determined after equilibration at 40% RH. The water content immediately after lyophilization ranged from 2.4% in lyophiles containing 43.1% HPMC to 6.1% for lyophiles containing 69.1% HPMC. After vacuum drying at 50°C, the water content of each formulation was reduced and became more consistent with values between 2% and 3% (w/w). After storage of lyophiles varying in HPMC percentage at 40% RH and 40°C, their water contents ranged from 8% to 10% (w/w) and did not differ significantly with the HPMC percentage. Previously, we reported the water content for lyophiles prepared from solutions containing 0.5% HPMC that were equilibrated at 40% RH and 40°C to be significantly higher than the value in Table 1 (first column).<sup>37</sup> Most of the discrepancy (~5%) stems from the fact that no carbonate correction was applied previously. Also, because one of the aims of the present study was to examine the effect of water content, larger sample sizes were employed in the present Karl Fischer analyses and other changes in sampling procedure were implemented in order to reduce possible moisture changes during sample manipulation. The present results for water content are believed to be more reliable.

Although water concentrations did not change significantly with an increase in HPMC percentage, an increase in the amount of HPMC did lead to a corresponding reduction in the solid-state Gly-Val concentration. The solid-state concentrations of Gly-Val (M)

**Table 1.** Weight Percentages of the Individual Components in Amorphous Lyophiles Prepared from Solutions Varying in the Amount of HPMC

HPMC in Solution (%w/v)	0.50%		1.00%		1.50%		2.00%		3.00%	
	w/w (%)	M	w/w (%)	M	w/w (%)	M	w/w (%)	M	w/w (%)	M
Gly-Phe-L-Asn-Gly	3.18	—	2.96	—	2.75	—	2.24	—	1.63	—
Gly-Val	10.8	0.806	7.52	0.562	5.61	0.419	4.56	0.340	3.30	0.246
Carbonate	23.4	—	16.3	—	12.1	—	9.86	—	7.14	—
Sodium	10.1	—	7.06	—	5.13	—	4.18	—	3.04	—
HPMC	43.1	—	57.4	—	64.8	—	69.2	—	76.1	—
TFA	0.977	—	0.517	—	0.511	—	0.386	—	0.302	—
Water content after drying	2.40	—	2.38	—	3.23	—	3.14	—	3.07	—
Water content @ 40% RH	8.43	—	8.36	—	9.37	—	9.75	—	8.65	—

Also included is the measured water content of lyophiles after drying in a vacuum oven at 50°C and after equilibration at 40% RH.

were estimated assuming a solid density of 1.3 g/mL. These concentrations were later used to calculate second-order rate constants for covalent amide-linked adduct formation to test the assumption in the model (Fig. 1) that this reaction is bimolecular.

Water contents in lyophiles containing a constant amount of HPMC [43.1% (w/w)] at 40% RH increased linearly with increasing RH (Fig. 2). Also shown are literature values for water content in films of HPMC alone<sup>46</sup> as a function of RH. The higher values found for lyophiles described in these experiments indicate that the peptides and carbonate buffer contribute substantially to the overall moisture uptake. To confirm that the absorption of water in HPMC films is similar to HPMC lyophiles, the water content of a lyophilized sample of the HPMC employed in this study was determined at 40% RH as indicated by the triangle in Figure 2. The similarity of this value to that previously reported in the literature confirms that the other formulation components contribute significantly to the water affinity in the present formulations.

### Reactant and Degradant Profiles

The identification and characterization of each the succinimide intermediates and subsequent degradants, including the hydrolysis products and covalent amide-linked adducts, have been previously described elsewhere.<sup>37</sup> The starting reactant, Gly-Phe-L-Asn-Gly, first undergoes deamidation to form the reactive L-succinimide intermediate. The L-succinimide intermediate partially racemizes in the amorphous solid as well as in solution to form a D-succinimide intermediate. Both succinimide isomers are then susceptible to nucleophilic attack at both the  $\alpha$ - and  $\beta$ -carbonyls. In the case wherein water is the nucleophile, isoaspartate (attack at the  $\alpha$ -carbonyl) and aspartate (attack at the  $\beta$ -carbonyl) residues replace the original asparagine residue. Likewise, the primary amine group at the N-terminus of Gly-Val can react with either carbonyl in both the D- and L-succinimide intermediates to form two different types of branched peptides (four different amide-linked adducts). In summary, a total of 10 degradants

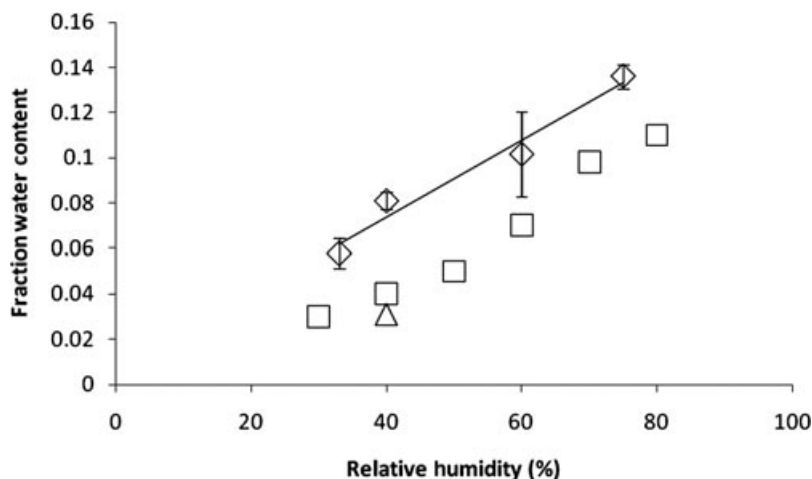


**Figure 2.** Increase in water content for the lyophiles containing constant HPMC (43.1%, w/w) and buffers when stored at different relative humidities [ $\diamond$ , error bars represent standard deviations ( $n = 3$ )] and water content for pure HPMC films<sup>45</sup> ( $\square$ ). The water content for a pure HPMC lyophile stored at 40% RH generated in the present study is also shown ( $\triangle$ ).

can be generated from the deamidation of the starting reactant Gly–Phe–L–Asn–Gly including the D- and L-succinimide intermediates, D- and L-diastereomers of isoaspartate and aspartate containing peptides, and four covalent and amide-linked Gly–Val adducts.

Under all the experimental conditions explored in this manuscript, both aspartyl and isoaspartyl peptides and covalent Gly–Val adducts were observed. We have previously examined the suitability of a kinetic model wherein all of the observed degradants proceed through a succinimide intermediate.<sup>37</sup> Using the Gly–Phe–L–Asn–Gly and its succinimide intermediate as the starting reactant and simultaneously fitting concentration profiles over time, it was confirmed that all degradants were produced through the succinimide intermediate.<sup>43</sup> However, given the focus of the present manuscript on effects of formulation and storage conditions on the overall reaction rate and the partitioning of the succinimide intermediate to form either hydrolysis products or covalent amide-linked adducts, individual degradant concentrations were pooled together into larger classes including “imides,” “aspartates,” and “adducts.” The advantage of grouping the degradants into larger categories is that more reliable rate constants could be generated from the higher concentrations of analytes produced. Shown in Figure 3 is a representative example of the data generated during the degradation of Gly–Phe–L–Asn–Gly lyophiles along with the fits obtained using Eqs. 1–4. Consistent with previous observations, the reaction scheme in Figure 1 and Eqs. 1–4 provided good simultaneous fits of concentration versus time data for reactant disappearance, product formation, and succinimide intermediate concentrations, which were

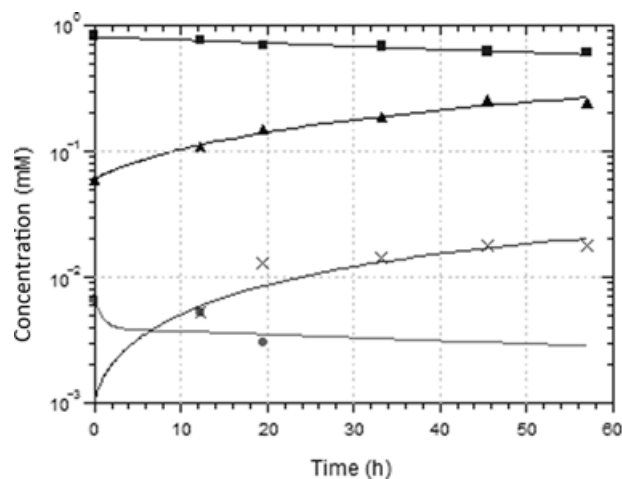


**Figure 3.** Semilogarithmic plots of concentration versus time for the degradation of Gly–Phe–L–Asn–Gly (■) to the succinimide intermediates (■) and the formation of hydrolysis products (▲) and covalent adducts (X) in lyophiles containing 76% HPMC stored at 40°C and 40% RH.

typically present at low, approximately steady-state concentrations over the time course of these studies.

### Reaction Kinetics with Varying HPMC Content

Shown in Figures 4a–4c are the concentration versus time profiles for the starting reactant Gly–Phe–L–Asn–Gly (a), the aspartates (b), and covalent Gly–Val adducts (c) in lyophiles containing various weight percentages of HPMC. The overlays of the fraction Gly–Phe–L–Asn–Gly remaining over time at various HPMC weight percentages were nearly superimposable (Fig. 4a), suggesting that increasing the amount of HPMC polymer diluent in the formulations had a negligible impact on the overall degradation rate. Similarly, no significant effect of HPMC content was discernible in Figure 4b, wherein the concentrations of aspartates over time at various HPMC weight percentages are displayed. The most significant impact of HPMC content can be observed in Figure 4c, wherein the fraction of covalent amide-linked adduct formation was clearly highest in the lyophiles with the lowest HPMC percentage. Decreasing rates of formation were observed as HPMC percentage was increased from 43% to 64%, above which there was a diminishing effect of further increases in HPMC content.

Pseudo-first-order rate constants for the various reaction steps depicted in Figure 1 and in Eqs. 1–4, generated from simultaneous fits to the data in Figure 4, are listed in Table 2. The rate constants for the rate-determining step in the deamidation of the starting reactant Gly–Phe–L–Asn–Gly (i.e., succinimide formation) did not change significantly as the weight percentage of HPMC increased, judging from the overlap of the 95% confidence limits. Similarly, the rate constants for aspartate formation showed no trend with increasing HPMC content. Only for covalent adduct formation were there significant differences in the pseudo-first-order rate constants. The decrease in covalent amide-linked adduct formation with increases in HPMC excipient concentration resulted in dramatic changes in the ratios of hydrolysis products to covalent adducts, as also evident in Table 2.

The rate constants and error bars for the 95% confidence limits shown in Table 2 are plotted against the weight percentage of HPMC in Figures 5a–5c. Visually, there appears to be a correlation between the rate constant for deamidation and HPMC content in Figure 5a, and a correlation coefficient from a linear fit of 0.88 was obtained, but based on the 95% confidence interval for the slope, this correlation was not significant. The individual rate constants for aspartate formation in Figure 5b are clearly scattered around the average value, confirming the lack of correlation between aspartate formation and HPMC content. The plot for rates of formation of covalent adducts decreased significantly with increasing amounts of

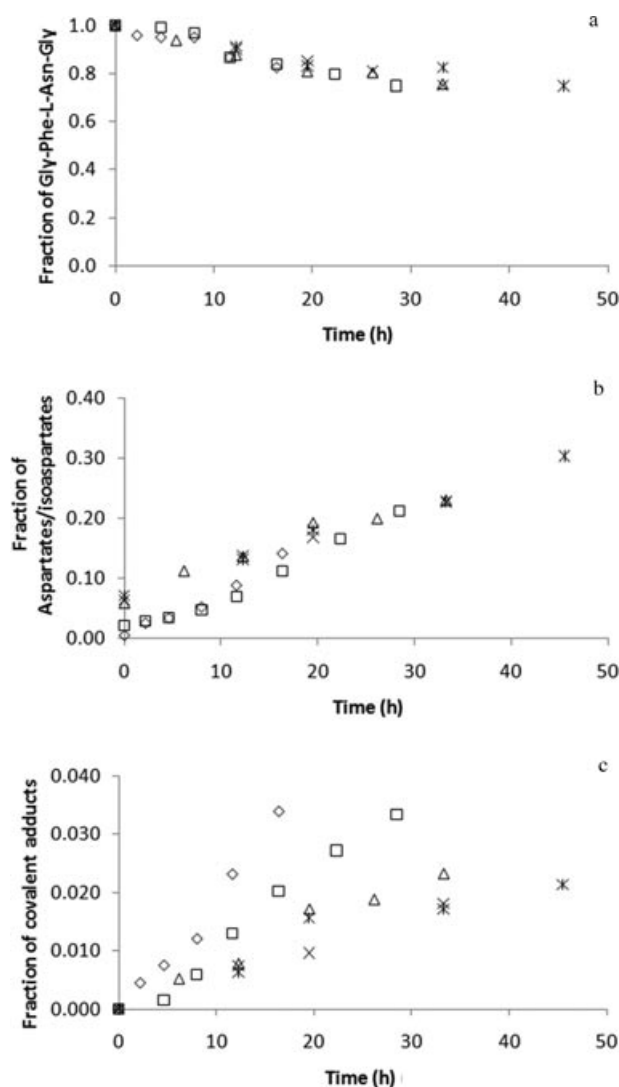


**Figure 4.** Concentration versus time profiles for the starting reactant Gly-Phe-L-Asn-Gly (a) and the formation of aspartates (b) and covalent Gly-Val adducts (c) in lyophiles containing various weight percentages of HPMC [43% ( $\diamond$ ), 56% ( $\square$ ), 64% ( $\triangle$ ), 69% ( $\times$ ), and 77% ( $*$ )] at 40°C/40% RH.

HPMC (Fig. 5c). Qualitatively, this behavior is consistent with the expected bimolecular nature of this reaction step coupled with the dilution of Gly-Val accompanying increases in HPMC content

(Table 1). Assuming that the reaction between Gly-Val and the succinimide intermediate is a second-order reaction and therefore dependent on the concentration of Gly-Val as indicated by Eq. 5,

$$\frac{\partial [\text{Adducts}]}{\partial t} = k_{\text{adducts}} [\text{Gly-Val}] [\text{Succinimide}] \quad (5)$$

and that the succinimide intermediate is at steady-state, Eq. 5 can be reduced to Eq. 6.

$$\frac{\partial [\text{Adducts}]}{\partial t} = k'_{\text{adducts}} [\text{Gly-Val}] \quad (6)$$

To further evaluate the dilution effects on the overall rate of adduct formation, a plot of the calculated second-order rate constant versus the effective concentration of Gly-Val in the lyophile was generated (Fig. 6). The calculated rate constants for  $k_{\text{adducts}}$  varied from 0.286 to 0.484  $\text{M}^{-1} \text{h}^{-1}$ , but fluctuated around the average value with no significant differences as determined by the overlap of their 95% confidence intervals, consistent with Eq. 5.

#### Reaction Kinetics with Varying Water Content

The qualitative effects of water content on the degradation of Gly-Phe-L-Asn-Gly and degradant formation can be seen in Figure 7a. At 33% RH, over 4000 h were needed to obtain approximately 10% degradation of the starting reactant compared with 75% RH when only 1 h was needed to achieve the same amount of degradation. The first-order rate constant for the deamidation of Gly-Phe-L-Asn-Gly trends upward from 5.8% to 10.2% water content and then plateaus from 10.2% to 13.6% water content (Fig. 8). No change was detected in the rate of deamidation from 10.2% to 13.6% water content, indicating that the plasticization effects of water on this reaction had reached a maximum.

Dramatic increases in the rates of degradant formation can be seen in Figures 7b and 7c as water is increased. Similar to the degradation of Gly-Phe-L-Asn-Gly, the required time to generate the same amount of degradants at 33% RH compared

**Table 2.** Pseudo-First-Order Rate Constants ( $\text{h}^{-1}$ ) Described in Eqs. 1–4 Using Data Generated from Lyophiles Containing Various Percentages of HPMC Stored at 40°C/40% RH

HPMC Content (w/w)	43%	57%	65%	69%	76%
Succinimide formation	0.0104 (0.008–0.013)	0.0069 (0.0031–0.011)	0.0074 (0.0051–0.0097)	0.0064 (0.0042–0.0085)	0.0062 (0.0028–0.0096)
Aspartate formation	1.35 (0.95–1.76)	0.83 (0.31–1.3)	1.10 (0.69–1.52)	1.24 (0.66–1.82)	1.15 (0.34–1.96)
Adduct formation	0.36 (0.26–0.47)	0.161 (0.077–0.25)	0.129 (0.092–0.166)	0.119 (0.074–0.165)	0.119 (0.057–0.18)
Ratio aspartates/adducts	3.8	5.1	8.5	10.4	9.7

Ratios of aspartate to covalent adduct formation rates are also shown. 95% Confidence intervals are reported in parentheses.

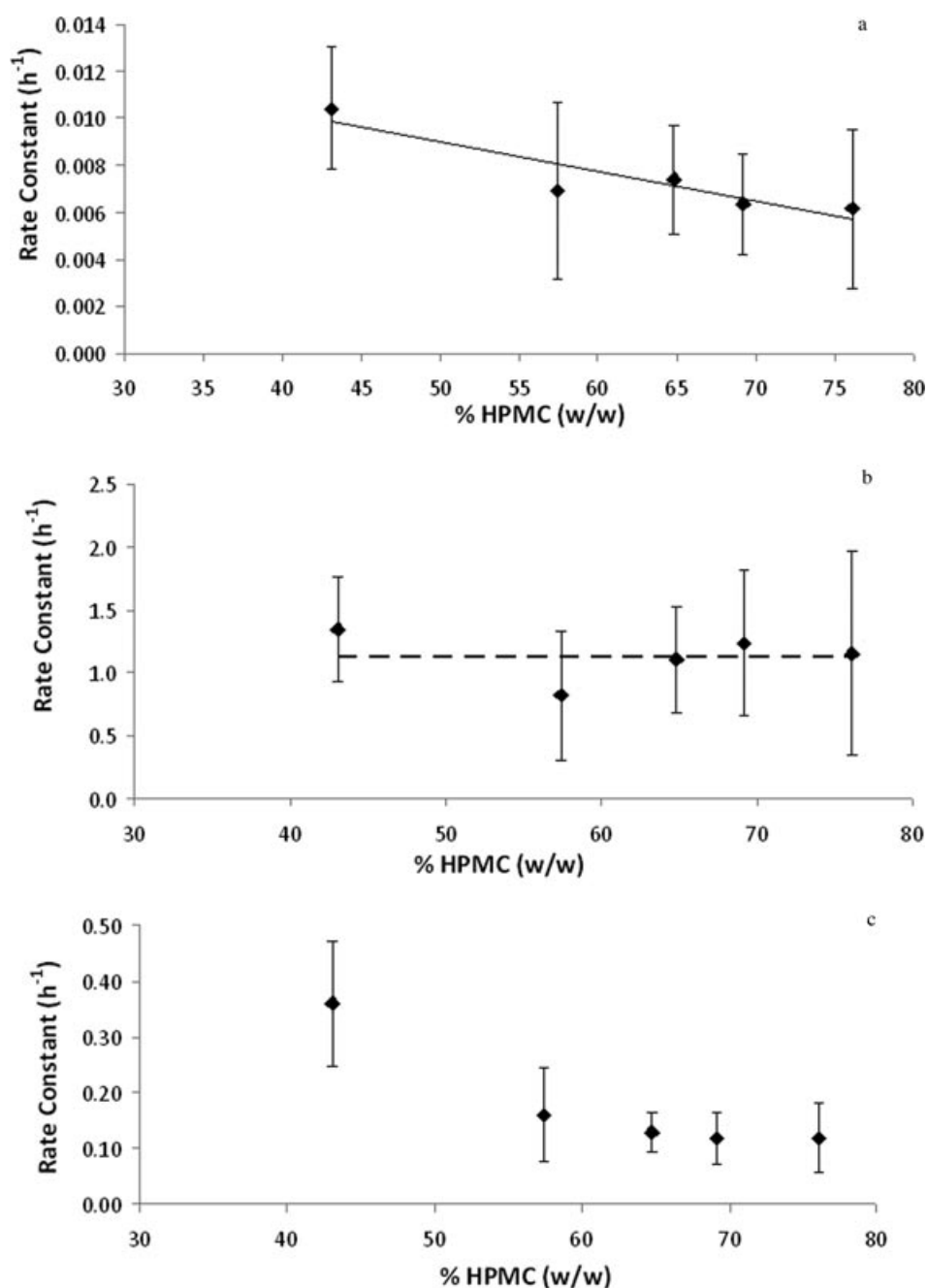


**Figure 5.** Pseudo-first-order rate constants for the deamidation of Gly-Phe-L-Asn-Gly (a), aspartate formation (b), and covalent adduct formation (c) in lyophiles as the weight percentage of HPMC increases. Dotted line in panel b represents the overall average of the individual rate constants. Error bars represent 95% confidence intervals.

with 75% RH was 2000 times longer. Figure 9 shows a semilogarithmic plot of the rate constants for formation of aspartate and adduct degradants at various water contents. The trend for aspartate formation with increasing water content resembled that for the formation of the succinimide intermediate. Increases in the rate of aspartate formation were observed from 5.8% to 10.2% water content, plateauing at 13.6%. Unlike the other reaction steps, adduct formation exhibited a bell-shaped profile. The rate increased from

5.8% to 8.1% water content and then decreased from 10.2% to 13.6%. The first-order rate constants for the degradation of the starting reactant and the formation of hydrolysis and adduct degradants are summarized in Table 3.

## DISCUSSION

Under basic conditions in both aqueous solutions and amorphous solids, the rate-limiting step in the deamidation of asparaginyl-containing proteins and



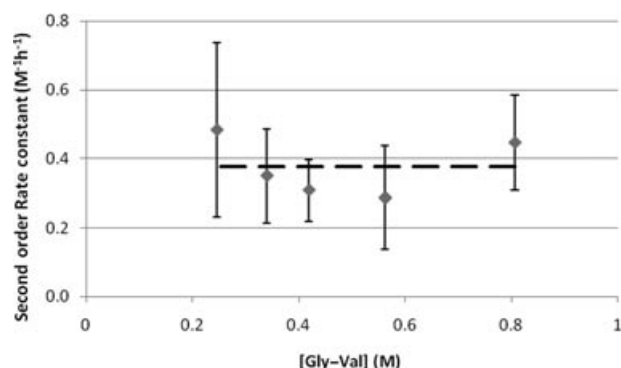


**Figure 6.** Plot of the calculated second-order rate constants for adduct formation as Gly-Val concentration is varied. The dashed line represents the overall average and error bars represent the 95% confidence intervals.

peptides is the formation of a reactive succinimide intermediate.<sup>24,35,36</sup> Generally, the succinimide then undergoes reaction with water at either its  $\alpha$ - or  $\beta$ -carbonyl to form isoaspartyl- and aspartyl-containing degradants.<sup>24</sup> Although this intermediate has been shown to be susceptible to attack by other nucleophiles in aqueous solutions, such as ammonia and substituted amine nucleophiles, these reactions seldom compete effectively with water, which is typically present at overwhelmingly higher concentrations.<sup>27</sup> Only at high nucleophile concentrations such as in concentrated ammonia buffers or when a nucleophilic substituent on the same molecule is situated in close proximity to the succinimide making possible an intramolecular reaction do such alternative pathways appear to be significant in aqueous solutions. However, in nonaqueous solvents or in amorphous lyophiles containing reduced water content, the situation appears to be more complicated, as both the number and complexity of degradants produced from asparaginyl deamidation increase substantially. Severs and Froland<sup>47</sup> recently attempted to stabilize a 31-amino-acid polypeptide drug candidate containing two asparaginyl residues that was susceptible to deamidation in aqueous solutions by formulating it in anhydrous DMSO. To their surprise, the degradation

rate did not decrease and multiple degradation products, including a variety of amide-linked dimers and multimers, were found. More recently, a study by Desfougères et al.<sup>48</sup> revealed that lysozyme dimerization was significant in freeze-dried powders stored in the dry state at 80°C and correlated with the concentration of succinimides. They proposed that dimerization could occur by the attack of a basic group of an amino acid side chain (e.g., lysine) on a neighboring protein molecule harboring a succinimide.<sup>48</sup>

By using a model system and a mechanism-based kinetic model, we have recently established that covalent amide-linked adduct formation in amorphous lyophiles could be attributed entirely to reactions involving a succinimide intermediate.<sup>37</sup> In this manuscript, we explored the influence of formulation and RH on the partitioning of the succinimide intermediate to produce either hydrolysis products or covalent amide-linked adducts.

Equations 1–4 based on the reaction mechanism outlined in Figure 1 were successfully utilized to simultaneously fit the concentration versus time data for reactant disappearance and the formation of both Gly-Val adducts and hydrolysis products (Figs. 4 and 7) as well as the succinimide concentrations that were typically present at a low steady-state level as illustrated by the example in Fig. 3. By applying a mechanism-based model, rate constants for each type of reaction step could be generated for every formulation and storage condition explored. These values are listed in Table 2 for formulations varying in HPMC content and stored at 40°C/40% RH and in Table 3 for lyophiles prepared from 0.5% (w/w) HPMC stored at 40°C and at varying RHs.

#### Dilution Effect by HPMC on Degradation of Gly-Phe-L-Asn-Gly and Degradant Formation

The two-step deamidation process illustrated in Figure 1 involving rate-determining succinimide formation followed by nucleophilic attack by either water or Gly-Val to yield aspartyl/isoaspartyl degradants or covalent amide-linked adducts, respectively, provides an opportunity to explore the effects of both

**Table 3.** Pseudo-First-Order Rate Constants ( $\text{h}^{-1}$ ) for Succinimide and Degradant Formation at Various Relative Humidities (and Water Contents) used to Generate Figures 8 and 9

Relative Humidity	33%	40%	60%	75%
Succinimide formation	$1.7 \times 10^{-5}$ ( $0.3 \times 10^{-5}$ – $3.1 \times 10^{-5}$ )	0.0104 (0.008–0.0130)	0.136 (0.029–0.243)	0.097 (0.080–0.114)
Aspartate formation	$1.9 \times 10^{-3}$ ( $0.35 \times 10^{-3}$ – $3.5 \times 10^{-3}$ )	1.35 (0.95–1.76)	4.5 (0.74–8.3)	2.35 (1.97–2.73)
Adduct formation	$1.5 \times 10^{-4}$ ( $0.23 \times 10^{-4}$ – $2.7 \times 10^{-4}$ )	0.360 (0.26–0.47)	0.51 (0.23–0.80)	0.044 (0.033–0.055)
Water content	5.80%	8.10%	10.2%	13.6%
Ratio aspartates/adducts	13	3.8	8.8	53

Ratios of aspartate to covalent adduct formation rates are also shown. 95% Confidence intervals are reported in parentheses.

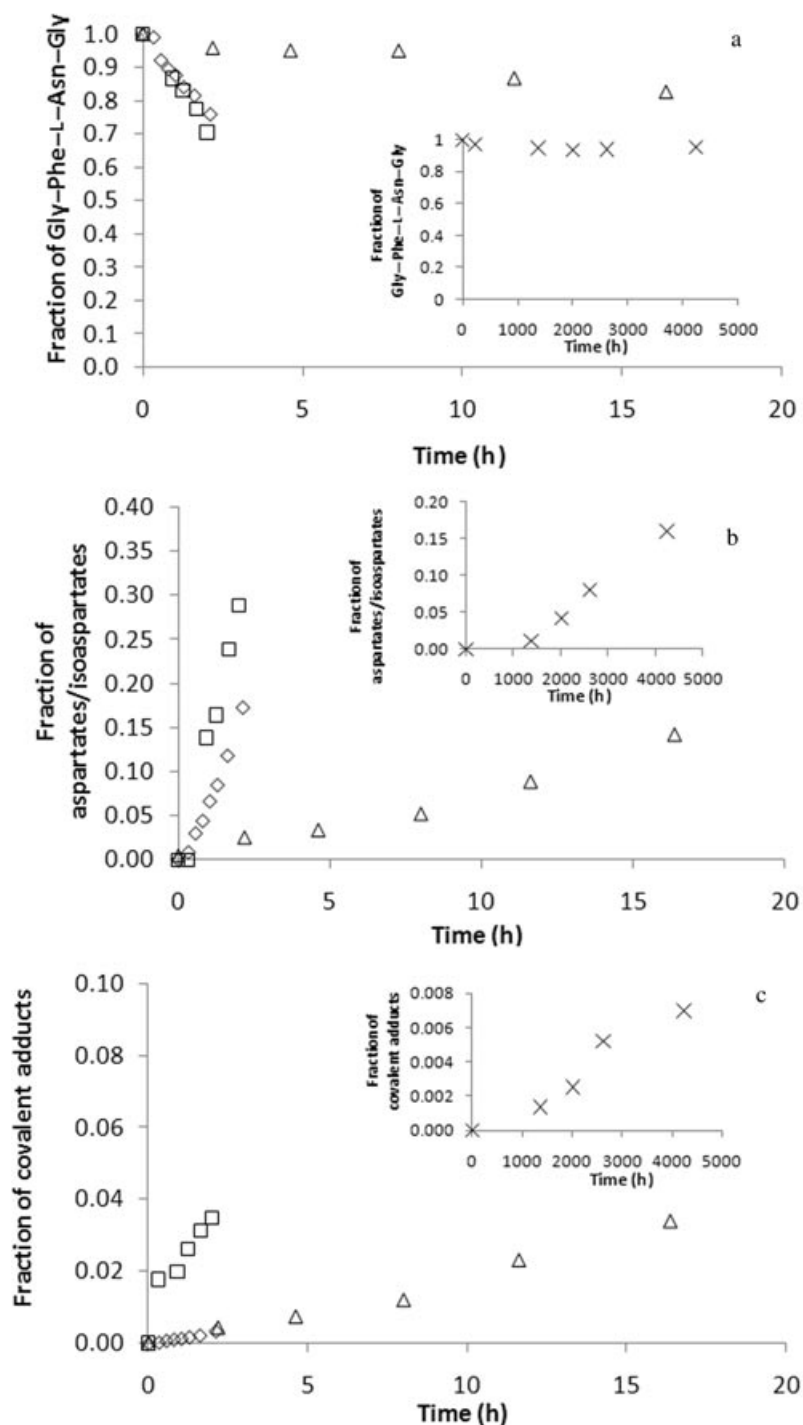


**Figure 7.** Concentration versus time profiles for the starting reactant Gly-Phe-L-Asn-Gly (a) and the aspartates (b) and covalent adducts (c) in lyophiles stored at 40°C and 33% RH (inset, X), 40% RH (Δ), 60% RH (□), and 75% RH (◇).

formulation and storage variables on these diverse reaction types. The first step involves the intramolecular attack of an asparaginyl nitrogen in the peptide backbone on the carbonyl of the asparagine side-chain amide resulting in succinimide formation accompanied by ammonia release. This reaction would be expected to exhibit first-order kinetics with

respect to the concentration of the starting peptide and therefore should be largely unaffected by the dilution accompanying increases in HPMC content in the formulation. Other consequences of increasing the HPMC content in the amorphous lyophiles that might affect the rate of deamidation could include possible alterations in water uptake at the same RH or

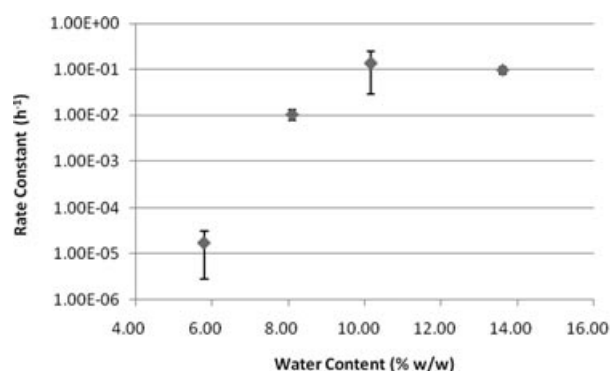


**Figure 8.** Semilogarithmic plot of deamidation rate constant in amorphous solids as water content is increased. Error bars represent 95% confidence intervals.

alterations in local mobility. Water molecules may participate in the reaction coordinate for succinimide formation by altering the relative stability of the transition state in relation to the ground state through hydrogen bonding.<sup>49</sup> Changes in local mobility accompanying increases in HPMC content might also influence succinimide formation, a reaction that has been shown to be highly dependent on segmental flexibility.<sup>50–53</sup>

The effect of percent HPMC content on succinimide formation, the overall rate-determining step in deamidation under the conditions of this study, is shown in Figure 5a. Although a negative slope was found for the rate constant for deamidation versus HPMC percentage, the overlap in 95% confidence limits in the data suggests that there is no statistically significant influence of HPMC content on this step. Also, the 95% confidence interval for the slope of the linear regression line included zero.

As shown in Table 1, increasing the amount of HPMC in amorphous lyophiles had no significant influence on the overall water content. Consistent with these results, Konno and Taylor<sup>41</sup> observed almost no increase in water uptake with HPMC content when lyophiles containing various amounts of HPMC (25%–85%, w/w) were exposed to 75% RH. Comparison of the equilibrium water content of the peptide containing lyophiles in this study with that for amorphous HPMC alone (Fig. 2) indicates that peptide and buffer salts accounted for approximately half of the water uptake (i.e., 4%) at 40% RH. Providing that the formulation components are molecularly dispersed, the nearly constant overall water content with increases in the HPMC content would be expected to have a negligible effect on the deamidation rates, consistent with the lack of a significant trend as shown in Figure 5a.

Although succinimide hydrolysis resulting in the formation of aspartyl and isoaspartyl peptides is a bimolecular reaction, in aqueous solutions the large

excess of water leads to pseudo-first-order reaction kinetics. Given the nearly constant water content in lyophiles as a function of HPMC percentage as reported in Table 1, pseudo-first-order kinetics would also be expected in these solid-state reactions. This was indeed the case, as illustrated by the nearly constant value for the pseudo-first-order hydrolysis rate constant as reported in Figure 5b.

Previously, Konno and Taylor<sup>41</sup> demonstrated that increasing the HPMC content in amorphous felodipine resulted in gradual increases in  $T_g$ , consistent with an antiplasticizing effect of HPMC. Attempts to obtain reliable values for  $T_g$  in the amorphous lyophiles of interest in this study were unsuccessful. However, the improved physical stability of these lyophiles in comparison with formulations of the same peptide components without HPMC (results not shown) and the absence of any evidence of physical collapse or crystallization of components when lyophiles were stored at 40°C and 40% RH are indicative of an inhibitory effect of HPMC on global (i.e., matrix) mobility. The absence of effects of increasing HPMC content on either the deamidation rate or the rate constant for succinimide hydrolysis could indicate either that changes in local mobility for relaxation processes that influence the reaction kinetics were small over the range of HPMC percentages explored or that neither of these reactions are significantly coupled to local mobility. The latter possibility is unlikely in view of the effects of increasing water content on these reactions, which contrast markedly with the HPMC results (*vide infra*).

Covalent adduct formation involves the bimolecular reaction of the succinimide with Gly–Val, a reaction that should be inhibited by the dilution effect resulting from increasing the amount of HPMC if the reactants are molecularly dispersed in these lyophile formulations. Increasing excipient content has been shown to be effective in reducing aggregation of proteins in amorphous sugars<sup>20</sup> and nucleation and recrystallization in polymers.<sup>54</sup> The plot for the rates of formation of covalent adducts decreased significantly with increasing amounts of HPMC (Fig. 5c), qualitatively conforming to the expected behavior given the bimolecular nature of this reaction step coupled with the dilution of Gly–Val (Table 1). To further evaluate the dilution effects, Figure 6 was generated to determine whether or not the reduction in covalent adduct formation could be quantitatively ascribed to changes in the Gly–Val concentrations when the model in Figure 1 was assumed. The calculated rate constants for  $k_{\text{adducts}}$  fluctuated around the average value with no apparent trend and no significant differences as determined by the overlap of their 95% confidence intervals.

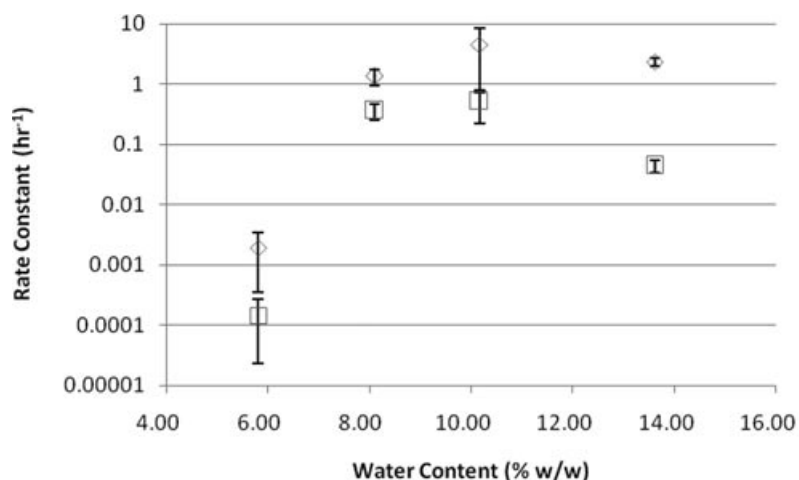


**Figure 9.** Semilogarithmic plot showing the effects of water content on the rate constants for aspartate (◇) and adduct (□) formation. Error bars represent 95% confidence intervals.

### Water Sensitivity—Dependence on the Reaction Step

As noted by others, water can play a myriad of roles in influencing chemical reactivity in amorphous solids.<sup>3,51,55–57</sup> It can function as a direct reactant, as in hydrolysis reactions; as a catalyst via solvation (e.g., hydrogen bonding) effects that may stabilize a transition state in relation to its ground state; as a plasticizer to increase local or global mobility; or as a solvent to solubilize reactants or alter local microenvironment pH or dielectric constant. Less appreciated but fairly certain in some cases is the likelihood that the nature of water's role will be dependent on the reaction type. For example, in the present study, the role of water as a direct reactant (i.e., nucleophile) applies only to succinimide hydrolysis. The plasticization effects of water may be more critical for the bimolecular steps governing the fate of the succinimide intermediate than for the intramolecular rate-determining reaction involved in its formation, given the need for translational mobility in the former, whereas only orientational mobility would appear to be necessary for the latter. Clearly ascribing the effect of water on amorphous reactivity to any one of the above possibilities may prove difficult.

Increases in RH from 33% to 75% resulted in linear increases in water content ranging from approximately 6% to 13% in amorphous lyophiles (Fig. 2). These increases in water content resulted in dramatic increases in the deamidation rate (i.e., succinimide formation) as displayed in Figure 8. A change in water content from 5.8% to 10.2% produced a striking increase in deamidation rate of nearly four orders-of-magnitude. Although we are unaware of other examples of such large increases in reactivity with a less than 5% increase in water content, others have reported that peptide deamidation rates in amorphous polymers can be highly sensitive to

moisture content.<sup>3,56</sup> Increasing water content from 10.2% to 13.6% (w/w) failed to increase the rate of succinimide formation further. Plateaus in the water-induced enhancement in chemical reactivity are common in the literature, and often indicate a reduction in the  $T_g$  of the system to a value near the storage temperature.<sup>29,56,58</sup> In the present study, partial collapse of the lyophiles was observed at 75% RH, suggesting that a reduction in the system  $T_g$  to a temperature close to 40°C did occur at this RH.

An increase in water content from 5.8% to 8.1% produced increases in both succinimide hydrolysis and covalent adduct formation of three or more orders-of-magnitude, as shown in Figure 9. For the hydrolysis reaction, this increase far exceeds that expected from the change in the solid-state water concentration, indicating that plasticization, transition-state solvation, or other solvent effects must play an important role. Although the rate constant for hydrolysis appears to reach a plateau at water contents above 8.1%, similar to the behavior of the succinimide formation step, the profile for the formation of covalent Gly–Val adducts is more complex. Despite the fact that succinimide hydrolysis might be expected to undergo greater acceleration than covalent adduct formation from increases in water content in the low-water-content region because water is a direct reactant in the case of hydrolysis, the opposite occurred. At lower water contents between 5.8% and 8.1%, the rate of amide-linked adduct formation increased more dramatically than the rate of hydrolysis, increasing by approximately 100-fold compared with a 24-fold increase in aspartate formation in this region. Strickley and Anderson<sup>30</sup> observed a similar phenomenon in their study of insulin degradation in lyophiles prepared from solutions at pH 2–5. Within this region, insulin degradation occurs via a cyclic anhydride intermediate formed at the A<sub>21</sub> terminal asparagine

residue. This intermediate can then undergo competing hydrolysis or covalent insulin dimer formation. They found that as water content increased the fraction of dimer formation in relation to hydrolysis increased. To account for this counterintuitive finding, they invoked free volume theory as originally developed by Cohen and Turnbull,<sup>59,60</sup> wherein the diffusion coefficient depends exponentially on the mean free volume available in the matrix and the permeant size. Smaller molecules, such as water, have significant mobility compared with larger peptide or protein molecules in rigid structures such as glasses. Although larger diffusants are severely restricted in their translational mobility in glasses at low water content, they undergo disproportionate increases in molecular mobility relative to a small molecule such as water in systems containing an added plasticizer.

Unlike the other two reaction pathways, the formation of covalent adducts exhibits a bell-shaped profile versus water content. The rate of adduct formation increased from 5.8% to 8.1% water content, with a flattening in the rate from 8.1% to 10.2%, followed by a decrease of approximately 10-fold from 10.2% to 13.6%. Bell-shape profiles in plots of degradation rate versus water content have been reported quite frequently,<sup>58</sup> and have been rationalized in the context of water's multiple roles in influencing reaction kinetics.<sup>58,61</sup> For example, plasticization effects leading to increased reactant mobility with increasing water content may be overshadowed by the dilution accompanying additional increases in water content.

Alternatively, increasing amounts of water in the amorphous lyophiles may induce or promote phase separation of one or more of the formulation components, leading to a reduction in the rate of covalent adduct formation. Increasing water content in polymers leads to water clustering due to self-association of water,<sup>62–64</sup> producing heterogeneity in water distribution. In HPMC at high moisture contents (>6%), water diffusivity increases are correlated with moisture-induced swelling.<sup>46</sup> These plasticization effects may promote redistribution of other small molecules in the formulation, particularly ionized species such as Gly–Val, which have a high affinity for water, as suggested by Figure 2.

Previous researchers have described phase separation in binary mixtures of HPMC with another polymer<sup>65</sup> or peptide.<sup>66</sup> Hussain et al.<sup>66</sup> employed multiple methods such as scanning electron microscopy, differential scanning calorimetry, and atomic force microscopy to detect phase separation between HPMC and cyclosporin A, noting that the degree of phase separation increased with the peptide concentration.<sup>66</sup> These observations suggest that phase separation in the present systems, particularly at high moisture contents, cannot be ruled out.

## CONCLUSION

This study examined the effects of changes in percentage of a polymeric excipient (HPMC) and water content on the degradants formed from a model asparaginyl peptide (Gly–Phe–L–Asn–Gly) in amorphous solids also containing an excess of Gly–Val and carbonate buffer and stored at 40°C. Deamidation of Gly–Phe–L–Asn–Gly in amorphous solids resulted in the formation of hydrolysis products (aspartates and isoaspartates) and covalent amide-linked adducts. In all formulations and storage conditions, the formation kinetics of aspartyl hydrolysis products and covalent adducts could be described by a mechanism-based model that assigned a central role to the succinimide intermediate. Increasing the percentage of HPMC (i.e., reactant dilution) did not significantly affect the overall degradation rate but did favor the formation of hydrolysis products over covalent amide-linked adducts, consistent with the bimolecular nature of covalent adduct formation. Increases in water content as RH was varied from 33% to 75% produced orders-of-magnitude increases in the rate constants for succinimide formation and hydrolysis with both becoming nearly constant at high water contents. A bell-shaped profile for the dependence of the rate of covalent adduct formation on water content was observed, a result that may be indicative of phase separation at higher RHs.

## REFERENCES

1. Duddu SP, Weller K. 1996. Importance of glass transition temperature in accelerated stability testing of amorphous solids: Case study using a lyophilized aspirin formulation. *J Pharm Sci* 85:345–347.
2. Wang W. 2000. Lyophilization and development of solid protein pharmaceuticals. *Int J Pharm* 203:1–60.
3. Lai M, Hageman MJ, Schowen RL, Topp EM. 1999. Chemical stability of peptides in polymers. 1. Effect of water on peptide deamidation in poly(vinyl alcohol) and poly(vinylpyrrolidone) matrices. *J Pharm Sci* 10:1073–1080.
4. Yoshioka S, Aso Y, Nakai Y, Kojima S. 1998. Effect of high molecular mobility of poly(vinyl alcohol) on protein stability of lyophilized gamma-globulin formulations. *J Pharm Sci* 87:147–151.
5. Hancock BC, Shamblin SL, Zografi G. 1995. Molecular mobility of amorphous pharmaceutical solids below their glass transition temperatures. *Pharm Res* 12:799–806.
6. Kawakami K, Pikal MJ. 2005. Calorimetric investigation of the structural relaxation of amorphous materials: Evaluating validity of the methodologies. *J Pharm Sci* 94:948–965.
7. Hancock BC, Shamblin SL. 2001. Molecular mobility of amorphous pharmaceuticals determined using differential scanning calorimetry. *Thermochim Acta* 380:95–107.
8. Liu J, Riggsbee DR, Pikal MJ. 2002. Dynamics of pharmaceutical amorphous solids: The study of enthalpy relaxation by isothermal microcalorimetry. *J Pharm Sci* 91:1853–1862.
9. Bhugra C, Shmeis R, Krill SL, Pikal MJ. 2008. Different measures of molecular mobility: Comparison between calorimetric and thermally stimulated current relaxation times below  $T_g$

- and correlation with dielectric relaxation times above  $T_g$ . *J Pharm Sci* 97:4498–4515.
10. Bhattacharya S, Suryanarayanan R. 2011. Molecular motions in sucrose–PVP and sucrose–sorbitol dispersions: I. Implications of global and local mobility on stability. *Pharm Res* 28:2191–2203.
  11. Duddu SP, Sokoloski TD. 1995. Dielectric analysis in the characterization of amorphous pharmaceutical solids. 1. Molecular mobility in poly(vinylpyrrolidone)–water systems in the glassy state. *J Pharm Sci* 84:773–776.
  12. Hancock BC, Dupuis Y, Thibert R. 1999. Determination of viscosity of an amorphous drug using thermomechanical analysis (TMA). *Pharm Res* 16:672–675.
  13. Yoshioka S, Aso Y, Kojima S. 1999. The effect of excipients on the molecular mobility of lyophilized formulations, as measured by glass transition temperature and NMR relaxation-based critical mobility temperature. *Pharm Res* 16:135–140.
  14. Williams ML, Landel RF, Ferry JD. 1955. Mechanical properties of substances of high molecular weight. 19. The temperature dependence of relaxation mechanisms in amorphous polymers and other glass-forming liquids. *J Am Chem Soc* 77:3701–3707.
  15. Sun WQ, Davidson P, Chan HS. 1998. Protein stability in the amorphous carbohydrate matrix: Relevance to anhydrobiosis. *Biochim Biophys Acta* 1425:245–254.
  16. Pikal MJ, Rigsbee D, Roy ML, Galreath D, Kovach KJ, Wang B, Carpenter JF, Cicerone MT. 2008. Solid state chemistry of proteins. II. The correlation of storage stability of freeze-dried human growth hormone (hGH) with structure and dynamics in the glassy solid. *J Pharm Sci* 97:5106–5121.
  17. Yoshioka S, Aso Y, Kojima S. 2001. Usefulness of the Kohlrausch–Williams–Watts stretched exponential function to describe protein aggregation in lyophilized formulations and the temperature dependence near the glass transition temperature. *Pharm Res* 18:256–260.
  18. Yoshioka S, Tajima S, Aso Y, Kojima S. 2003. Inactivation and aggregation of  $\beta$ -galactosidase in lyophilized formulation described by Kohlrausch–Williams–Watts stretched exponential function. *Pharm Res* 20:1655–1660.
  19. Pikal MJ, Rigsbee DR. 1997. The stability of insulin in crystalline and amorphous solids: Observation of greater stability for the amorphous form. *Pharm Res* 14:1379–1387.
  20. Chang L, Shepherd D, Sun J, Tang X, Pikal MJ. 2005. Effect of sorbitol and residual moisture on the stability of lyophilized antibodies: Implications for the mechanism of protein stabilization in the solid state. *J Pharm Sci* 94:1445–1455.
  21. Yoshioka S, Miyazaki T, Aso Y, Kawanishi T. 2007. Significance of local mobility in aggregation of beta-galactosidase lyophilized with trehalose, sucrose or stachyose. *Pharm Res* 24(9):1660–1667.
  22. Shamblyn SL, Hancock BC, Pikal MJ. 2006. Coupling between chemical reactivity and structural relaxation in pharmaceutical glasses. *Pharm Res* 23:2254–2268.
  23. Cicerone MT, Soles CL. 2004. Fast dynamics and stabilization of proteins: Binary glasses of trehalose and glycerol. *Biophys J* 86:3836–3845.
  24. Geiger T, Clarke S. 1987. Deamidation, isomerization, and racemization at asparaginyl and aspartyl residues in peptides. Succinimide-linked reactions that contribute to protein degradation. *J Biol Chem* 262:785–794.
  25. Shen H, Tsuchida S, Tamai K, Sato K. 1993. Identification of cysteine residues involved in disulfide formation in the inactivation of glutathione transferase P-form by hydrogen peroxide. *Arch Biochem Biophys* 300:137–141.
  26. Winterbourn CC, Metodewa D. 1999. Reactivity of biologically important thiol compounds with superoxide and hydrogen peroxide. *Free Rad Biol Med* 27:322–328.
  27. Dehart MP, Anderson BD. 2007. The role of the cyclic imide in alternate degradation pathways for asparagine-containing peptides and proteins. *J Pharm Sci* 96(10):2667–2685.
  28. Oliyai C, Borchardt RT. 1993. Chemical pathways of peptide degradation. IV. Pathways, kinetics, and mechanism of degradation of an aspartyl residue in a model hexapeptide. *Pharm Res* 10:95–102.
  29. Strickley RG, Anderson BD. 1996. Solid-state stability of human insulin I. Mechanism and the effect of water on the kinetics of degradation in lyophiles from pH 2–5 solutions. *Pharm Res* 13:1142–1153.
  30. Strickley RG, Anderson BD. 1997. Solid-state stability of human insulin II. Effect of water on reactive intermediate partitioning in lyophiles from pH 2–5 solutions: Stabilization against covalent dimer formation. *J Pharm Sci* 86:645–653.
  31. Zale SE, Klibanov AM. 1986. Why does ribonuclease irreversibly inactivate at high temperatures? *Biochemistry* 25:5432–5444.
  32. Luo D, Smith SW, Anderson BD. 2005. Kinetics and mechanism of the reaction of cysteine and hydrogen peroxide in aqueous solution. *J Pharm Sci* 94:304–316.
  33. Luo D, Anderson BD. 2006. Kinetics and mechanism for the reaction of cysteine with hydrogen peroxide in amorphous polyvinylpyrrolidone lyophiles. *Pharm Res* 23:2239–2253.
  34. Qiu Z, Stowell JG, Morris KR, Byrn SR, Pinal R. 2005. Kinetic study of the Maillard reaction between metoclopramide hydrochloride and lactose. *Int J Pharm* 303:20–30.
  35. Oliyai C, Patel J, Carr L, Borchardt RT. 1994. Solid-state stability of lyophilized formulations of an asparaginyl residue in a model hexapeptide. *J Parenter Sci Technol* 48:67–173.
  36. Song Y, Schowen RL, Borchardt RT, Topp EM. 2001. Effect of ‘pH’ on the rate of asparagine deamidation in polymeric formulations: ‘pH’-rate profile. *J Pharm Sci* 90:141–156.
  37. DeHart MP, Anderson BD. 2011. Kinetics and mechanisms of deamidation and covalent amide-linked adduct formation in amorphous lyophiles of a model asparagine-containing peptide. *Pharm Res* [Epub ahead of print].
  38. Chang LL, Shepherd D, Sun J, Ouellette D, Grant KL, Tang XC, Pikal MJ. 2005. Mechanism of protein stabilization by sugars during freeze-drying and storage: Native structure preservation, specific interaction, and/or immobilization in a glassy matrix? *J Pharm Sci* 94:1427–1444.
  39. Yoshioka M, Hancock BC, Zografi G. 1995. Inhibition of indomethacin crystallization in poly(vinylpyrrolidone) coprecipitates. *J Pharm Sci* 84:983–986.
  40. Yamashita K, Nakate T, Okimoto K, Ohike A, Tokunaga Y, Ibuki R, Higaki K, Kimura T. 2003. Establishment of new preparation method for solid dispersion formulation of tacrolimus. *Int J Pharm* 267:79–91.
  41. Konno H, Taylor LS. 2008. Ability of different polymers to inhibit the crystallization of amorphous felodipine in the presence of moisture. *Pharm Res* 25(4):969–978.
  42. Nyamweya N, Hoag SW. 2000. Assessment of polymer–polymer interactions in blends of HPMC and film forming polymers by modulated temperature differential scanning calorimetry. *Pharm Res* 17:625–631.
  43. DeHart MP, Anderson BD. 2012. Development of a comprehensive kinetic model for the succinimide mediated formation of racemic hydrolysis products and covalent adducts accompanying peptide deamidation in amorphous solids. *J Pharm Sci* (in press).
  44. Carotenuto A, Dell’Isola M. 1996. An experimental verification of saturated salt solution-based humidity fixed points. *Int J Thermophys* 17:1423–1439.
  45. Mitchell J, J. 1951. Karl Fischer reagent titration. *Anal Chem* 23:1069–1075.
  46. Lakshmana FL, Kok PJA, Frijlink HW, Vromans H, Maarschalk KV. 2010. Gas permeation related to the

- moisture sorption in films of glassy hydrophilic polymers. *J Appl Polym Sci* 116:3310–3317.
47. Severs JC, Froland WA. 2008. Dimerization of a PACAP peptide analogue in DMSO via asparagine and aspartic acid residues. *J Pharm Sci* 97:1246–1256.
48. Desfougères Y, Jardin J, Lechevalier V, Pezennec S, Nau F. 2011. Succinimidyl residue formation in hen egg-white lysozyme favors the formation of intermolecular covalent bonds without affecting its tertiary structure. *Biomacromolecules* 12:156–166.
49. Catak S, Monard G, Aiyente V, Ruiz-Lopez MF. 2006. Reaction mechanism of deamidation of asparaginyl residues in peptides: Effect of solvent molecules. *J Phys Chem A Mol Spectrosc Kinet Environ Gen Theory* 110(27):8354–8365.
50. Clarke S. 1987. Propensity for spontaneous succinimide formation from aspartyl and asparaginyl residues in cellular proteins. *Int J Peptide Protein Res* 30:808–821.
51. Hageman MJ. 1992. Water sorption and solid state stability of proteins. In *Stability of protein pharmaceuticals: Chemical and physical pathways of protein degradation*; Ahern TJ, Manning MC, Eds. New York: Plenum.
52. Xie M, Aube J, Borchardt RT, Morton M, Topp EM, Vander Velde D, Schowen RL. 2000. Reactivity toward deamidation of asparagine residues in beta-turn structures. *J Pept Res* 56(3):165–171.
53. Xie M, Shahrokh Z, Kadkhodayan M, Henzel WJ, Powell MF, Borchardt RT, Schowen RL. 2003. Asparagine deamidation in recombinant human lymphotoxin: Hindrance by three-dimensional structures. *J Pharm Sci* 92(4):869–880.
54. Yoshioka S, Aso Y, Otsuka T, Kojima S. 1995. Water mobility in poly(ethylene glycol)-, poly(vinylpyrrolidone)-, and gelatin-water systems, as indicated by dielectric relaxation times, spin-lattice relaxation time, and water activity. *J Pharm Sci* 84:1072–1077.
55. Bell LN, Hageman MJ. 1994. Differentiating between the effects of water activity and glass transition dependent mobility on a solid state chemical reaction: Aspartame degradation. *J Agric Food Chem* 40:873–879.
56. Lai MC, Hageman MJ, Schowen RL, Borchardt RT, Laird BB, Topp EM. 1999. Chemical stability of peptides in polymers. 2. Discriminating between solvent and plasticizing effects of water on peptide deamidation in poly(vinyl pyrrolidone). *J Pharm Sci* 88:1081–1089.
57. Shalaev EY, Zografi G. 1996. How does residual water affect the solid-state degradation of drugs in the amorphous state? *J Pharm Sci* 85:1137–1141.
58. Lai MC, Topp EM. 1999. Solid-state chemical stability of proteins and peptides. *J Pharm Sci* 88:489–500.
59. Cohen MH, Turnbull D. 1959. Molecular transport in liquids and glasses. *J Chem Phys* 31(5):1164–1169.
60. Ganesh K, Nagarajan R, Duda JL. 1992. Rate of gas transport in glassy polymers: A free volume based predictive model. *Ind Eng Chem Res* 31:746–755.
61. Chang BS, Reeder G, Carpenter JF. 1996. Development of a stable freeze-dried formulation of recombinant human interleukin-1 receptor antagonist. *Pharm Res* 13:243–249.
62. Xiang T-X, Anderson BD. 2005. Distribution and effect of water content on molecular mobility in poly(vinylpyrrolidone) glasses: A molecular dynamics simulation. *Pharm Res* 22:1205–1214.
63. Marque G, Neyertz S, Verdu J, Prunier V, Brown D. 2008. Molecular dynamics simulation study of water in amorphous kapton. *Macromolecules* 41:3349–3362.
64. Kucukpinar E, Doruker P. 2004. Effect of absorbed water on oxygen transport in EVOH matrices. A molecular dynamics study. *Polymer* 45:3555–3564.
65. Sakellariou P, Rowe RC. 1994. Phase-separation and polymer interactions in aqueous poly(vinyl alcohol) hydroxypropyl methylcellulose blends for tablet coating. *J Macromol Sci Pure A* 31:1201–1208.
66. Hussain S, Grandy DB, Reading M, Craig DQ. 2004. A study of phase separation in peptide-loaded HPMC films using *T*(zero)-modulated temperature DSC, atomic force microscopy, and scanning electron microscopy. *J Pharm Sci* 93:1672–1681.